



## Study of Two Dimensional Boundary Layer Flow of a Thin Film Second Grade Fluid with Variable Thermo-Physical Properties in Three Dimensions Space

Noor Saeed Khan<sup>a</sup>

<sup>a</sup>Department of Mathematics, Abdul Wali Khan University, Mardan, 23200, Khyber Pakhtunkhwa, Pakistan

**Abstract.** The formation of three dimensional study from two dimensional study due to high intensified magnetic field is investigated for a thin film second-grade fluid with variable fluid properties. The effects of Soret, Dufour, thermophoresis, thermal radiation and viscous dissipation are taken into account in the problem. Similarity transformations are employed to convert the governing equations into dimensionless form which have been solved by using homotopy analysis method (HAM). Quite real results are achieved with the help of emerging parameters which are shown through different graphs for velocities, temperature and concentration profiles.

### 1. Introduction

A current resisting at right angle to both the electric and magnetic fields is known as Hall current. Hall current is generated when strong magnetic field is applied. Therefore magnetohydrodynamic has great importance due to its various applications like materials processing, MHD energy generators, cancer therapy, biomedical flow and separation devices. Khan *et al.* [1] discussed the boundary layer flow problem in which the high intensified magnetic field effect is investigated taken into account the Brownian motion and thermophoresis effects. Rafiq *et al.* [2] examined the peristaltic flow of viscous nanofluid in a channel with compliant walls in the presence of Hall and ion-slip effects. Khan *et al.* [3] analyzed the heat and mass transfer flow with the effects of thermophoresis and thermal radiation in MHD thin film second grade fluid of variable properties. Filippini *et al.* [4] investigated the ferromagnetic in a magnetic transmission gear adopting a homogenized hysteretic model able to include eddy current and hysteresis losses in two dimensional laminated materials for iron poles. Khan *et al.* [5] worked on the effective thermal conductivity and viscosity of the nanofluid in which the Brownian motion effect on the effective thermal conductivity is included through KKL (Koo-Klein-streuer-Li) correlation. Hajmohammadi and Ali [6] assessed the effectiveness of the magnetic field on nanofluids in a rotary system described by a stationary housing and the rotating cylinder in which the magnetic field can be imposed by the environment or applied as controlled parameter. Bilal and Ramzan [7] presented the unsteady two-dimensional flow of mixed convection and nonlinear thermal radiation in the presence of water-based carbon nanotubes over the vertically convected

---

2010 Mathematics Subject Classification. Primary 74A15

Keywords. MHD; Boundary layer; Hall Current Effect; Thermophoresis; Thin Film; Second-Grade; Variable Viscosity and Thermal Conductivity; Heat and Mass Transfer; Thermal Radiation; Viscous Dissipation; Stretching Sheet; Homotopy Analysis Method.

Received: 08 January 2018; Revised: 21 February 2019; Accepted: 05 March 2019

Communicated by Maria Alessandra Ragusa

Email address: noorsaedkhan@tak@gmail.com (Noor Saeed Khan)

stretched sheet embedded in a Darcy' Forchheimer porous media using Saffman's proposed model for the suspension of fine dust particles in the nanofluid in which strong magnetic field is applied normal to the flow. Fersadou *et al.* [8] investigated the mixed convection heat transfer and entropy generation analysis for Cu-water nanofluid inside two interacting open cavities by heating or cooling the right and the left walls of each cavity at uniform but different heat flux densities. Khan and Zuhra [9] investigated the two dimensional magnetohydrodynamic unsteady flow and heat transfer in a thin film second grade nanofluid embedded with graphene nanoparticles past a stretching sheet. They proved that graphene nanoparticles have continuous electrical conductivity since the charge carrier movement in graphene bears extremely high values compared to the available nanomaterials. Atashafrooz [10] studied the buoyancy force effects on the MHD mixed convection nanofluid flow and entropy generation over an inclined step in an inclined duct where the inclined step leads to the flow separation in duct and affects the hydrodynamic and thermal behaviors. Palwasha *et al.* [11] analyzed the application of strong MHD on heat and mass transfer flow of second grade fluid past a stretching sheet in which quite interestingly it is shown that two dimensional study converts into three dimensional case due to Hall current effect. Khan *et al.* [12] performed a theoretical study on the behavior of transformed internal energy in a magnetohydrodynamic Maxwell nanofluid flow past a stretching sheet along with Arrhenius activation energy and chemical reaction. Zuhra *et al.* [13] investigated the effect of MHD on the second grade nanofluid heat and mass transfer flow containing nanoparticles and gyrotactic microorganisms. Bidemi and Ahamed [14] considered two dimensional unsteady Casson magneto-nanofluid flow past an inclined plate embedded in a porous medium with Soret-Dufour effects by showing that the applied magnetic field slow down the motion of the fluid. Khan *et al.* [15] analyzed the slip flow of Eyring-Powell nanoliquid film containing graphene nanoparticles and heat transfer in the presence of magnetohydrodynamics to prove that temperature decreased with increasing magnetic field strength. Daniel *et al.* [16] focused on the impacts of slip conditions on the two-dimensional unsteady mixed convection flow of electrical magnetohydrodynamic nanofluid past a stretching sheet in the presence of thermal radiation, viscous dissipation, and chemical reaction. Zangoee *et al.* [17] discussed the nanofluid flow between two stretchable and rotating disks with homogeneous-heterogeneous chemical reactions and Joule heating in the presence of magnetic field and thermal radiation. The other MHD and non-MHD studies can be seen in the references [18–23].

Navier-Stokes equations can be seen in modeling of the fluid flows in various problem due to their extensive applications. Benbernou [24] established a Serrin-type regularity criterion in terms of pressure for Leray weak solutions to the Navier-Stokes equations. Involving fluid flow, Gala *et al.* [25] presented a study that deals with the blow-up criterion for the hydrodynamic system modeling the flow of three-dimensional nematic liquid crystal materials. Magnetohydrodynamics equations represent the flow of an electrically conducting fluid in the presence of magnetic field, which essentially needs to consider the interaction between magnetic fields and fluid conductors of electricity. To solve such equations in three dimensions, Benbernou *et al.* [26] presented logarithmically improved regularity criterion for the incompressible magnetohydrodynamics equation in terms of the derivative of the pressure in one direction. Gala and Ragusa [27] used logarithmically improved regularity criteria for supercritical quasi-geostrophic equations in Orlicz-Morrey spaces. Moreover, this criterion is in terms of the norm of the solution in a Orlicz-Morrey space.

The Boussinesq equation is one of the important subjects for researches in nonlinear sciences. However, similar to the classic Navier-Stokes equations, the question of global regularity of the weak solutions of the 3D Boussinesq equations still remains a big open problem. There are a huge literatures on the incompressible Boussinesq equations. Attempting Boussinesq equations, Gala and Ragusa [28] developed logarithmically improved regularity criterion for the Boussinesq equations in Besov spaces with negative indices. In another note, Gala *et al.* [29] considered the regularity problem under the critical condition to the Boussinesq equations with zero heat conductivity. Mehdene *et al.* [30] reported the logarithmical regularity criterion of the three-dimensional Boussinesq equations in terms of pressure. Similarly, Gala and Ragusa [31] proved a logarithmic regularity criterion for the 2D MHD equations without magnetic diffusion in terms of the magnetic field in homogeneous Besov space  $B_{\infty, \infty}^0$ . Working on the stretching flow, Khan *et al.* [32] discussed the boundary layer movement of a non-Newtonian second grade fluid through a porous medium past a stretching surface with heat transfer under the consideration of thin film. Zuhra *et al.* [33] analyzed the steady non-Newtonian nanofluids flow containing graphene nanoparticles on stretch-

ing sheet by comparing the behavior of two non-Newtonian nanofluids namely Casson and Williamson. Khan *et al.* [34] discussed the effect of strong applied magnetic field on thin film flow of second grade fluid with entropy generation past a stretching sheet. Khan *et al.* [35] investigated the effect of inclined magnetic field on flow and heat transfer containing graphene nanoparticles past a stretching sheet. Khan *et al.* [36] reported the mixed convection in gravity-driven non-Newtonian nanoliquid thin films (Casson and Williamson) flow containing both nanoparticles and gyrotactic microorganisms along a convectively heated vertical solid surface with the actively controlled nanofluid model boundary conditions to investigate the liquids thermodynamics analytically.

Due to strong applications of magnetohydrodynamics, it is the author interest to investigate the influence of strong applied magnetic field on mixed convection heat and mass transfer thin film flow with fluid variable properties past a stretching sheet using Homotopy Analysis Method (HAM) [37]. The influences of the emerging parameters on velocities, temperature and concentration profiles are shown in figures and explained.

## 2. Methods

### 2.1. Basic equations

The mixed convective steady MHD laminar boundary layer flow of an incompressible and electrically conducting second grade thin film fluid with temperature dependent viscosity and thermal conductivity past a stretching sheet in two dimensions is considered.  $x$ -axis is along the surface of the stretching sheet and  $y$ -axis is normal to it. Leading edge of the stretching surface is in the direction of  $z$ -axis as shown in Fig. 1.

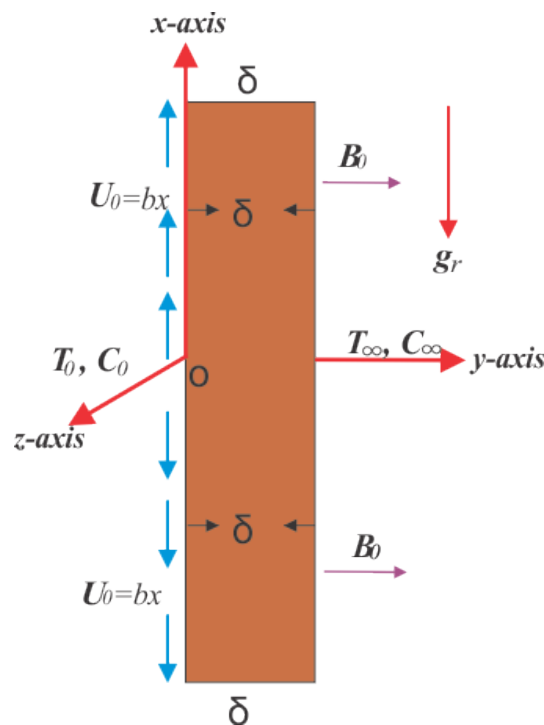


Figure 1: Problem geometry.

A strong magnetic field is applied in the direction normal to the sheet. Due to high intensity of magnetic field a force in  $z$ -direction is generated which causes a cross flow in the  $z$ -direction consequently the flow

becomes three-dimensional. Applying Ohm’s law in the general form involving Hall current as in [11] is

$$\vec{j} + \frac{\omega_e \tau_e}{B_0} \times (\vec{j} \times \vec{B}) = \sigma (\vec{E} + \vec{V} \times \vec{B}), \tag{1}$$

where  $\vec{j} = (j_x, j_y, j_z)$  is the current density vector,  $\vec{V} = (u, v, w)$  is the velocity vector,  $\vec{E}$  is the intensity vector of the electric field,  $\vec{B} = (0, B_0, 0)$  is the magnetic induction vector,  $\omega_e$ ,  $\sigma$ ,  $\tau_e$  and  $e$  are electron frequency, electrical conductivity, electron collision time and charge of electron respectively. Due to the absence of imposed or polarization voltage on the flow field, the electric field vector  $\vec{E} = 0$ . Following the above assumptions, the Ohm’s law in general form for a weakly ionized gases results in  $j_y = 0$  everywhere in the flow so comparing the  $x, z$  components in Eq. (1) and simplifying for the current density components  $j_x$  and  $j_z$  as

$$j_x = \frac{\sigma B_0}{1 + m^2} (mu - w), \tag{2}$$

$$j_z = \frac{\sigma B_0}{1 + m^2} (mw + u), \tag{3}$$

where  $u, v$  and  $w$  are the components of the velocity vector  $\vec{V}$  along  $(x, y$  and  $z)$ -axes respectively and  $m = \omega_e \tau_e$  is Hall parameter.

The governing equations of the problem are

$$\frac{\partial u}{\partial x} + \frac{\partial v}{\partial y} = 0, \tag{4}$$

$$u \frac{\partial u}{\partial x} + v \frac{\partial u}{\partial y} = \frac{1}{\rho} \frac{\partial}{\partial y} \left( \mu(T) \frac{\partial u}{\partial y} \right) + \frac{\alpha_1}{\rho} \left[ u \frac{\partial^3 u}{\partial x \partial y^2} + v \frac{\partial^3 u}{\partial y^3} + \frac{\partial u}{\partial x} \frac{\partial^2 u}{\partial y^2} - \frac{\partial u}{\partial y} \frac{\partial^2 u}{\partial x \partial y} + \frac{\partial w}{\partial y} \frac{\partial^2 w}{\partial x \partial y} + \frac{\partial w}{\partial x} \frac{\partial^2 w}{\partial y^2} \right] + g_r \beta_T (T - T_\infty) + g_r \beta_C (C - C_\infty) - \frac{\sigma B_0^2 (1 + mw)}{\rho (1 + m^2)}, \tag{5}$$

$$u \frac{\partial w}{\partial x} + v \frac{\partial w}{\partial y} = \frac{1}{\rho} \frac{\partial}{\partial y} \left( \mu(T) \frac{\partial w}{\partial y} \right) + \frac{\alpha_1}{\rho} \left[ u \frac{\partial^3 w}{\partial x \partial y^2} + v \frac{\partial^3 w}{\partial y^3} \right] + \frac{\sigma B_0^2 (mu - w)}{\rho (1 + m^2)}, \tag{6}$$

$$\rho c_p \left( u \frac{\partial T}{\partial x} + v \frac{\partial T}{\partial y} \right) = \frac{\partial}{\partial y} \left( K(T) \frac{\partial T}{\partial y} \right) - \frac{\partial q_r}{\partial y} + \mu(T) \left[ \frac{\partial u}{\partial y} \right]^2 + \alpha_1 \left[ u \frac{\partial u}{\partial y} \frac{\partial^2 u}{\partial x \partial y} + v \frac{\partial u}{\partial y} \frac{\partial^2 u}{\partial y^2} + v \frac{\partial w}{\partial y} \frac{\partial^2 w}{\partial y^2} + u \frac{\partial w}{\partial y} \frac{\partial^2 w}{\partial y^2} \right] + \sigma B_0^2 (u^2 + w^2) + \frac{D_m K_T}{C_s} \frac{\partial^2 C}{\partial y^2}, \tag{7}$$

$$u \frac{\partial C}{\partial x} + v \frac{\partial C}{\partial y} = \frac{D_m \partial^2 C}{\partial y^2} + \frac{D_m K_T}{T_m} \frac{\partial^2 T}{\partial y^2} - \frac{\partial (V_T C)}{\partial y}, \tag{8}$$

where  $\mu(T) = \frac{\mu_0}{1 - \gamma \left( \frac{T - T_0}{T_{ref} \left( \frac{bx^2}{2v} \right)} \right)}$  represents the temperature reliant viscosity having  $\mu_0$  as the liquid viscosity at

reference temperature  $T_0$  and  $\gamma$  is the strength of interrelation between  $\mu$  and  $T$ ,  $K(T) = K_\infty \left( 1 - \varepsilon \left( \frac{T - T_0}{T_{ref} \left( \frac{bx^2}{2v} \right)} \right) \right)$  shows the temperature reliant thermal conductivity having  $K_\infty$  as the thermal conductivity of the fluid far away from the surface of the sheet,  $\varepsilon$  represents the variable thermal conductivity parameter [11],  $\alpha_1 (>0)$  represents the material parameter,  $\rho$  represents the density,  $\beta_T$  represents the coefficient of thermal expansion,  $\beta_C$  represents the coefficient of volumetric expansion,  $c_p$  represents the specific heat at constant

pressure  $P$ ,  $g_r$  represents the gravitational acceleration,  $T$  represents the fluid temperature,  $C$  represents the concentration,  $q_r$  represents the radiative heat flux,  $D_m$  represents the molecular diffusivity,  $K_T$  represents the thermal diffusion ratio,  $T_m$  represents the mean fluid temperature,  $T_\infty$  represents the fluid temperature far away from the surface of the sheet,  $C_\infty$  represents the fluid concentration far away from the surface of the sheet,  $C_{sus}$  represents the absorption susceptibility,  $V_T (= -\frac{k_1 v}{T_{ref}} \frac{\partial T}{\partial y})$  represents the thermophoretic velocity in which  $k_1$  is the thermophoretic coefficient,  $\nu = \frac{\mu}{\rho}$  represents the kinematic viscosity of the second grade fluid and  $T_{ref}$  represents constant reference temperature [11].

Initially the slit is fixed with the origin. An external force is applied to the slit to make it stretch at the rate  $b$  in the positive  $x$ -direction with velocity  $U_0$ . Considering the stretching velocity along positive  $x$ -axis as  $U_0 = bx$ ,

where  $b > 0$  is the stretching rate. The surface temperature

$$T_s(x) = T_0 - T_{ref} \left[ \frac{bx^2}{2\nu} \right]$$

is assumed to vary with the distance  $x$  from the slit in which  $T_0$  is the temperature at the slit such that  $0 \leq T_{ref} \leq T_0$ . Similarly the surface concentration

$$C_s(x) = C_0 - C_{ref} \left[ \frac{bx^2}{2\nu} \right]$$

is varying with the distance  $x$  from the slit in which  $C_0$  is the concentration at the slit and  $C_{ref}$  is the reference concentration such that  $0 \leq C_{ref} \leq C_0$ .

The boundary conditions are represented as

$$u = U_0, \quad v = 0, \quad w = 0, \quad T = T_0, \quad C = C_0 \quad \text{at} \quad y = 0, \tag{9}$$

$$\frac{\partial u}{\partial y} = \frac{\partial w}{\partial y} = \frac{\partial T}{\partial y} = 0, \quad v = \frac{d\delta}{dx}, \quad T = T_\infty, \quad C = C_\infty \quad \text{at} \quad y = \delta, \tag{10}$$

where  $\delta$  is the thickness of the second grade liquid film. By Rosseland approximation [11], the radiative heat flux is defined as

$$q_r = -\frac{4\sigma_1}{3k_2} \frac{\partial T^4}{\partial y}, \tag{11}$$

where  $\sigma_1$  and  $k_2$  are the Stefan-Boltzmann constant and the mean absorption coefficient respectively. By taking assumption that the differences in temperature within the flow are such that  $T^4$  can be expressed as a linear combination of the temperature and using the Taylor's theorem to expand  $T^4$  about  $T_\infty$  and neglecting higher order terms, one obtains

$$T^4 = 4T_\infty^3 T - 3T_\infty^4, \tag{12}$$

so

$$\frac{\partial q_r}{\partial y} = -\frac{16T_\infty^3 \sigma_1}{3k_2} \frac{\partial^2 T}{\partial y^2}. \tag{13}$$

Applying the transformations for nondimensional variables  $f, g, \theta, \phi$  and similarity variable  $\zeta$  as

$$u = bx f'(\zeta), \quad v = -(bv)^{\frac{1}{2}} f(\zeta), \quad w = bx g(\zeta), \quad \zeta = \left[ \frac{b}{\nu} \right]^{\frac{1}{2}} y, \tag{14}$$

$$T(x) = T_0 - T_{ref} \left[ \frac{bx^2}{2\nu} \right] \theta(\zeta), \quad C(x) = C_0 - C_{ref} \left[ \frac{bx^2}{2\nu} \right] \phi(\zeta), \quad \beta = \left[ \frac{b}{\nu} \right]^{\frac{1}{2}} \delta, \tag{15}$$

where  $\beta$  represents the non-dimensional parameter for the thickness of the second grade fluid film. It is easy to see that mass conservation Eq. (4) is identically satisfied through Eq. (14). By using Eqs. (14) and (15), the basic governing Eqs. (5-10) of the problem are transformed into the following six ordinary

differential equations (16-21)

$$f''' + (1 + \wedge\theta) [ff'' - f'^2] + \gamma_1(1 + \wedge\theta) [2ff'' - f'^2 - ff'' + g'^2 + gg''] + Gr(1 + \wedge\theta)\theta + Gm(1 + \wedge\theta)\phi - \frac{M(1 + \wedge\theta)(f' + mg)}{1 + m^2} = 0, \quad (16)$$

$$g'' + (1 + \wedge\theta) [fg' - f'g] + \gamma_1(1 + \wedge\theta) [f'g'' - fg'''] + \frac{M(1 + \wedge\theta)(mf' - g)}{1 + m^2} = 0, \quad (17)$$

$$(1 + Nr + \varepsilon\theta)\theta'' - Pr(2f'\theta - f\theta') + Br [M(\rho^2 + g^2) + (\rho'^2 + g'^2) + \gamma_1 [f'(f'f'' - ff''')] + f'g'^2 - fg'g''] + PrDu\phi'' = 0, \quad (18)$$

$$\phi'' + Sc(f - \tau\theta')\phi' + Sc(Sr - \tau\phi)\theta'' - 2Scf\phi = 0, \quad (19)$$

$$f = g = 0, \quad f' = \theta = \phi = 1 \quad \text{at} \quad \zeta = 0, \quad (20)$$

$$f' = g' = \theta' = \phi' = 0 \quad \text{at} \quad \zeta = \beta, \quad (21)$$

where prime (') represents the derivative with respect to  $\zeta$ ,  $\wedge = \gamma(T_0 - T_\infty)$  represents the variable viscosity parameter,  $\gamma_1 = \frac{\alpha_1\beta^2}{\rho\delta^2}$  represents the second grade fluid parameter,  $Gr = \frac{g_r\beta_T(T_0 - T_\infty)\delta^2}{\nu\beta^2}$  represents the thermal Grashof number,  $Gm = \frac{g_r\beta_C(C_0 - C_\infty)\delta^2}{\nu\beta^2}$  represents the solutal Grashof number,  $M = \frac{\sigma B_0^2\delta^2}{\rho\nu\beta^2}$  represents the magnetic field parameter,  $Nr = \frac{16T_\infty^3\sigma_1}{3k_2K}$  represents the thermal radiation parameter,  $Sc = \frac{\nu}{D_m}$  represents the Schmidt number,  $Sr = \frac{D_m K_T(T_0 - T_\infty)}{\nu T_m(C_0 - C_\infty)}$  represents the Soret number,  $\tau = -\frac{k_1(T_0 - T_\infty)}{T_{ref}}$  represents the thermophoretic parameter,  $Pr = \frac{\mu_0 c_p}{K}$  represents the Prandtl number,  $Br = \frac{\mu U_0^2}{K(T_0 - T_\infty)}$  represents the Brinkman number and  $Du = \frac{D_m K_T(C_\infty - C_0)}{C_{sus} \nu c_p (T_\infty - T_0)}$  represents the Dufour number. For  $\gamma_1 = 0$ , the present study corresponds to viscous fluid case.

### 3. Solution of the Problem by Homotopy Analysis Method

Applying the suitable initial approximations to satisfy the boundary conditions and auxiliary linear operators for velocity, temperature and concentration in the following form

$$f_0(\zeta) = \zeta, \quad g_0(\zeta) = 1, \quad \theta_0(\zeta) = 1, \quad \phi_0(\zeta) = 1, \quad (22)$$

$$L_f = f''', \quad L_g = g'', \quad L_\theta = \theta'', \quad L_\phi = \phi''. \quad (23)$$

The following properties are satisfied with the linear operators

$$L_f[C_1 + C_2\zeta + C_3\zeta^2] = 0, \quad L_g[C_4 + C_5\zeta] = 0, \quad L_\theta[C_6 + C_7\zeta] = 0, \quad L_\phi[C_8 + C_9\zeta] = 0, \quad (24)$$

where  $C_i (i = 1-9)$  are the arbitrary constants.

3.1. Zeroth-order deformation problems

Introducing the nonlinear operator  $\mathfrak{N}$  as

$$\begin{aligned} \mathfrak{N}_f[f(\zeta, p), g(\zeta, p), \theta(\zeta, p), \phi(\zeta, p)] &= \frac{\partial^3 f(\zeta, p)}{\partial \zeta^3} + (1 + \wedge \theta(\zeta, p)) \left[ f(\zeta, p) \frac{\partial^2 f(\zeta, p)}{\partial \zeta^2} - \left( \frac{\partial f(\zeta, p)}{\partial \zeta} \right)^2 \right] + \\ \gamma_1 (1 + \wedge \theta(\zeta, p)) &\left[ 2 \frac{\partial f(\zeta, p)}{\partial \zeta} \frac{\partial^3 f(\zeta, p)}{\partial \zeta^3} - \left( \frac{\partial^2 f(\zeta, p)}{\partial \zeta^2} \right)^2 - f(\zeta, p) \frac{\partial^4 f(\zeta, p)}{\partial \zeta^4} + \left( \frac{\partial g(\zeta, p)}{\partial \zeta} \right)^2 + g(\zeta, p) \frac{\partial^2 g(\zeta, p)}{\partial \zeta^2} \right] + \\ Gr(1 + \wedge \theta(\zeta, p))\theta(\zeta, p) &+ Gm(1 + \wedge \theta(\zeta, p))\phi(\zeta, p) - \frac{M(1 + \wedge \theta(\zeta, p))}{1 + m^2} \left[ \frac{\partial f(\zeta, p)}{\partial \zeta} + mg(\zeta, p) \right], \end{aligned} \quad (25)$$

$$\begin{aligned} \mathfrak{N}_g[f(\zeta, p), g(\zeta, p), \theta(\zeta, p)] &= \frac{\partial^2 g(\zeta, p)}{\partial \zeta^2} + (1 + \wedge \theta(\zeta, p)) \left[ f(\zeta, p) \frac{\partial g(\zeta, p)}{\partial \zeta} - \frac{\partial f(\zeta, p)}{\partial \zeta} g(\zeta, p) \right] + \\ \gamma_1 (1 + \wedge \theta(\zeta, p)) &\left[ \frac{\partial f(\zeta, p)}{\partial \zeta} \frac{\partial^2 g(\zeta, p)}{\partial \zeta^2} - f(\zeta, p) \frac{\partial^3 g(\zeta, p)}{\partial \zeta^3} \right] + \frac{M(1 + \wedge \theta(\zeta, p))}{1 + m^2} \left[ \frac{m \partial f(\zeta, p)}{\partial \zeta} - g(\zeta, p) \right], \end{aligned} \quad (26)$$

$$\begin{aligned} \mathfrak{N}_\theta[f(\zeta, p), \theta(\zeta, p)] &= (1 + Nr + \varepsilon \theta(\zeta, p)) \frac{\partial^2 \theta(\zeta, p)}{\partial \zeta^2} - Pr \left[ 2 \frac{\partial f(\zeta, p)}{\partial \zeta} \theta(\zeta, p) - f(\zeta, p) \frac{\partial \theta(\zeta, p)}{\partial \zeta} \right] \\ + Br &\left[ M \left[ \left( \frac{\partial f(\zeta, p)}{\partial \zeta} \right)^2 + \left( g(\zeta, p) \right)^2 \right] + \left[ \left( \frac{\partial^2 f(\zeta, p)}{\partial \zeta^2} \right)^2 + \left( \frac{\partial g(\zeta, p)}{\partial \zeta} \right)^2 \right] \right] + \\ \gamma_1 Br &\left[ \frac{\partial^2 f(\zeta, p)}{\partial \zeta^2} \left( \frac{\partial f(\zeta, p)}{\partial \zeta} \frac{\partial^2 f(\zeta, p)}{\partial \zeta^2} - f(\zeta, p) \frac{\partial^3 f(\zeta, p)}{\partial \zeta^3} \right) + \frac{\partial f(\zeta, p)}{\partial \zeta} \left( \frac{\partial g(\zeta, p)}{\partial \zeta} \right)^2 - f(\zeta, p) \frac{\partial g(\zeta, p)}{\partial \zeta} \frac{\partial^2 g(\zeta, p)}{\partial \zeta^2} \right] + PrDu \frac{\partial^2 \phi(\zeta, p)}{\partial \zeta^2}, \end{aligned} \quad (27)$$

$$\begin{aligned} \mathfrak{N}_\phi[f(\zeta, p), \theta(\zeta, p), \phi(\zeta, p)] &= \frac{\partial^2 \phi(\zeta, p)}{\partial \zeta^2} + Sc \left[ f(\zeta, p) - \tau \frac{\partial \theta(\zeta, p)}{\partial \zeta} \right] \frac{\partial \phi(\zeta, p)}{\partial \zeta} + Sc \left[ Sr - \tau \phi(\zeta, p) \right] \frac{\partial^2 \theta(\zeta, p)}{\partial \zeta^2} \\ &- 2Sc \frac{\partial f(\zeta, p)}{\partial \zeta} \phi(\zeta, p), \end{aligned} \quad (28)$$

where  $p$  is an embedding parameter such that  $p \in [0, 1]$ .

The zeroth-order deformation equations are constructed as

$$(1 - p)L_f[f(\zeta, p) - f_0(\zeta)] = p\hbar \mathfrak{N}_f[f(\zeta, p), g(\zeta, p), \theta(\zeta, p), \phi(\zeta, p)], \quad (29)$$

$$(1 - p)L_g[g(\zeta, p) - g_0(\zeta)] = p\hbar \mathfrak{N}_g[f(\zeta, p), g(\zeta, p), \theta(\zeta, p)], \quad (30)$$

$$(1 - p)L_\theta[\theta(\zeta, p) - \theta_0(\zeta)] = p\hbar \mathfrak{N}_\theta[f(\zeta, p), g(\zeta, p), \theta(\zeta, p)], \quad (31)$$

$$(1 - p)L_\phi[\phi(\zeta, p) - \phi_0(\zeta)] = p\hbar \mathfrak{N}_\phi[f(\zeta, p), \theta(\zeta, p), \phi(\zeta, p)], \quad (32)$$

where  $\hbar$  denotes the auxiliary nonzero parameter.

Eq. (29) has the boundary conditions

$$f(0, p) = 0, \quad f'(0, p) = 1, \quad f'(\beta, p) = 0. \quad (33)$$

Eq. (30) has the boundary conditions

$$g(0, p) = 0, \quad g'(\beta, p) = 0. \quad (34)$$

Eq. (31) has the boundary conditions

$$\theta(0, p) = 1, \quad \theta'(\beta, p) = 0. \quad (35)$$

Similarly Eq. (32) has the boundary conditions

$$\phi(0, p) = 1, \quad \phi'(\beta, p) = 0. \tag{36}$$

Noting the following results

$$p = 0 \Rightarrow f(\zeta, 0) = f_0(\zeta) \quad \text{and} \quad p = 1 \Rightarrow f(\zeta, 1) = f(\zeta), \tag{37}$$

$$p = 0 \Rightarrow g(\zeta, 0) = g_0(\zeta) \quad \text{and} \quad p = 1 \Rightarrow g(\zeta, 1) = g(\zeta), \tag{38}$$

$$p = 0 \Rightarrow \theta(\zeta, 0) = \theta_0(\zeta) \quad \text{and} \quad p = 1 \Rightarrow \theta(\zeta, 1) = \theta(\zeta). \tag{39}$$

Similarly

$$p = 0 \Rightarrow \phi(\zeta, 0) = \phi_0(\zeta) \quad \text{and} \quad p = 1 \Rightarrow \phi(\zeta, 1) = \phi(\zeta). \tag{40}$$

$f(\zeta, p)$  becomes  $f_0(\zeta)$  to  $f(\zeta)$  when  $p$  assumes the values from 0 to 1.  $g(\zeta, p)$  becomes  $g_0(\zeta)$  to  $g(\zeta)$  when  $p$  has the values from 0 to 1. Similarly,  $\theta(\zeta, p)$  becomes  $\theta_0(\zeta)$  to  $\theta(\zeta)$  when  $p$  assumes the values from 0 to 1. Exactly in the same manner for  $p = 0$ ,  $\phi(\zeta, 0) = \phi_0(\zeta)$  and for  $p = 1$ ,  $\phi(\zeta, 1) = \phi(\zeta)$ . Using Taylor series expansion and Eqs. (37-40), one develops

$$f(\zeta, p) = f_0(\zeta) + \sum_{m=1}^{\infty} f_m(\zeta)p^m, \quad f_m(\zeta) = \frac{1}{m!} \frac{\partial^m f(\zeta, p)}{\partial p^m} \Big|_{p=0}, \tag{41}$$

$$g(\zeta, p) = g_0(\zeta) + \sum_{m=1}^{\infty} g_m(\zeta)p^m, \quad g_m(\zeta) = \frac{1}{m!} \frac{\partial^m g(\zeta, p)}{\partial p^m} \Big|_{p=0}, \tag{42}$$

$$\theta(\zeta, p) = \theta_0(\zeta) + \sum_{m=1}^{\infty} \theta_m(\zeta)p^m, \quad \theta_m(\zeta) = \frac{1}{m!} \frac{\partial^m \theta(\zeta, p)}{\partial p^m} \Big|_{p=0}, \tag{43}$$

$$\phi(\zeta, p) = \phi_0(\zeta) + \sum_{m=1}^{\infty} \phi_m(\zeta)p^m, \quad \phi_m(\zeta) = \frac{1}{m!} \frac{\partial^m \phi(\zeta, p)}{\partial p^m} \Big|_{p=0}. \tag{44}$$

The convergence of the series is strongly dependent on  $\hbar$ . Suppose  $\hbar$  is chosen in such a way that the series in Eqs. (41-44) converge at  $p = 1$ , then Eqs. (41-44) result in

$$f(\zeta) = f_0(\zeta) + \sum_{m=1}^{\infty} f_m(\zeta), \tag{45}$$

$$g(\zeta) = g_0(\zeta) + \sum_{m=1}^{\infty} g_m(\zeta), \tag{46}$$

$$\theta(\zeta) = \theta_0(\zeta) + \sum_{m=1}^{\infty} \theta_m(\zeta), \tag{47}$$

$$\phi(\zeta) = \phi_0(\zeta) + \sum_{m=1}^{\infty} \phi_m(\zeta). \tag{48}$$

3.2. *m*th order deformation problem

By taking *m* times derivative with respect to *p* of Eqs. (29) and (33), then dividing by *m!* and substituting *p* = 0, yield the below simplifications

$$L_f[f_m(\zeta) - \chi_m f_{m-1}(\zeta)] = \hbar \mathfrak{R}_m^f(\zeta), \tag{49}$$

$$f_m(0) = f_m''(\beta) = f_m'(0) = 0, \tag{50}$$

$$\begin{aligned} \mathfrak{R}_m^f(\zeta) &= f_{m-1}''' + \sum_{k=0}^{m-1} [f_{m-1-k} f_k'' - f_{m-1-k}' f_k'] + \wedge \sum_{k=0}^{m-1} \theta_{m-1-k} \sum_{l=0}^k [f_{k-l} f_l'' - f_{k-l}' f_l'] + \\ &\gamma_1 \sum_{k=0}^{m-1} [2f_{m-1-k}' f_k''' - f_{m-1-k}'' f_k'' - f_{m-1-k} f_k^{iv} + g_{m-1-k}' g_k'' + g_{m-1-k} g_k'''] + \\ &\gamma_1 \wedge \sum_{k=0}^{m-1} \theta_{m-1-k} \sum_{l=0}^k [2f_{k-l}' f_l''' - f_{k-l}'' f_l'' - f_{k-l} f_l^{iv} + g_{k-l}' g_l'' + g_{k-l} g_l'''] + Gr \theta_{m-1} + \wedge Gr \sum_{k=0}^{m-1} \theta_{m-1-k} \theta_k + \\ &Gm \phi_{m-1} + \wedge Gm \sum_{k=0}^{m-1} \phi_{m-1-k} \phi_k - \frac{M}{1+m^2} [f_{m-1}' + m g_{m-1}] - \frac{\wedge M}{1+m^2} \sum_{k=0}^{m-1} [f_{m-1-k}' \theta_k - m g_{m-1-k} \theta_k]. \end{aligned} \tag{51}$$

By taking *m* times derivative with respect to *p* of Eqs. (30) and (34), then dividing by *m!* and substituting *p* = 0, yield the below simplifications

$$L_g[g_m(\zeta) - \chi_m g_{m-1}(\zeta)] = \hbar \mathfrak{R}_m^g(\zeta), \tag{52}$$

$$g_m(0) = g_m'(\beta) = 0, \tag{53}$$

$$\begin{aligned} \mathfrak{R}_m^g(\zeta) &= g_{m-1}'' + \sum_{k=0}^{m-1} [f_{m-1-k} g_k' - f_{m-1-k}' g_k] + \wedge \sum_{k=0}^{m-1} \theta_{m-1-k} \sum_{l=0}^k [f_{k-l} g_l' - f_{k-l}' g_l] + \gamma_1 \sum_{k=0}^{m-1} [f_{m-1-k}' g_k'' - f_{m-1-k} g_k'''] \\ &+ \wedge \gamma_1 \sum_{k=0}^{m-1} \theta_{m-1-k} \sum_{l=0}^k [f_{k-l}' g_l'' - f_{k-l} g_l'''] + \frac{M}{1+m^2} [m f_{m-1}' - g_{m-1}] + \frac{\wedge M}{1+m^2} \sum_{k=0}^{m-1} [m f_{m-1-k}' \theta_k - g_{m-1-k} \theta_k]. \end{aligned} \tag{54}$$

By taking *m* times derivative with respect to *p* of Eqs. (31) and (35), then dividing by *m!* and substituting *p* = 0, develop the below simplifications

$$L_\theta[\theta_m(\zeta) - \chi_m \theta_{m-1}(\zeta)] = \hbar \mathfrak{R}_m^\theta(\zeta), \tag{55}$$

$$\theta_m(0) = \theta_m'(\beta) = 0, \tag{56}$$

$$\begin{aligned} \mathfrak{R}_m^\theta(\zeta) &= (1 + Nr) \theta_{m-1}'' + \varepsilon \sum_{k=0}^{m-1} [\theta_{m-1-k} \theta_k''] - Pr \sum_{k=0}^{m-1} [2f_{m-1-k}' \theta_k - f_{m-1-k} \theta_k'] + \\ &Br [M \sum_{k=0}^{m-1} (f_{m-1-k}' f_k' + g_{m-1-k} g_k') + \sum_{k=0}^{m-1} [f_{m-1-k}'' f_k'' + g_{m-1-k}' g_k']] \\ &\gamma_1 Br [\sum_{k=0}^{m-1} f_{m-1-k}'' \sum_{l=0}^k (f_{k-l}' f_l'' - f_{k-l} f_l''') + \sum_{k=0}^{m-1} f_{m-1-k}' \sum_{l=0}^k (g_{k-l}' g_l') - \sum_{k=0}^{m-1} f_{m-1-k} \sum_{l=0}^k (g_{k-l}' g_l'')] \\ &+ Pr Du \phi_{m-1}''. \end{aligned} \tag{57}$$

Similarly by taking  $m$  times derivative with respect to  $p$  of Eqs. (32) and (36), then dividing by  $m!$  and substituting  $p = 0$ , develop the below simplifications

$$\mathcal{L}_\phi[\phi_m(\zeta) - \chi_m \phi_{m-1}(\zeta)] = \hbar \mathfrak{R}_m^\phi(\zeta), \tag{58}$$

$$\phi_m(0) = \phi'_m(\beta) = 0, \tag{59}$$

$$\mathfrak{R}_m^\phi(\zeta) = \phi''_{m-1} + Sc \sum_{k=0}^{m-1} [f_{m-1-k} \phi'_k] - Sc\tau \sum_{k=0}^{m-1} [\theta'_{m-1-k} \phi'_k] + ScSr\theta''_{m-1} - Sc\tau \sum_{k=0}^{m-1} [\phi_{m-1-k} \theta''_k] - 2Sc \sum_{k=0}^{m-1} [f'_{m-1-k} \phi_k], \tag{60}$$

$$\chi_m = \begin{cases} 0, & m \leq 1 \\ 1, & m > 1. \end{cases} \tag{61}$$

If  $f_m^*(\zeta)$ ,  $g_m^*(\zeta)$ ,  $\theta_m^*(\zeta)$  and  $\phi_m^*(\zeta)$  are the particular solutions, then the general solutions of Eqs. (49), (52), (55) and (58) are

$$f_m(\zeta) = f_m^*(\zeta) + C_1 + C_2\zeta + C_3\zeta^2, \tag{62}$$

$$g_m(\zeta) = g_m^*(\zeta) + C_4 + C_5(\zeta), \tag{63}$$

$$\theta_m(\zeta) = \theta_m^*(\zeta) + C_6 + C_7\zeta, \tag{64}$$

$$\phi_m(\zeta) = \phi_m^*(\zeta) + C_8 + C_9\zeta. \tag{65}$$

#### 4. Results and Discussion

The non-dimensional Eqs. (16-21) are solved through the symbolic computer package MATHEMATICA employing HAM package. The effects of embedded parameters on velocities ( $f(\zeta)$ ,  $g(\zeta)$ ), temperature  $\theta(\zeta)$  and concentration  $\phi(\zeta)$  profiles are shown in Figures (6-11), (12-15) and (16-18) respectively. The physical description of the problem is displayed in Fig. 1. Following Liao [37], the  $\hbar$ -curves are drawn to evaluate the range of values of  $\hbar$  that generates a convergent series solution. Therefore, for the admissible values of  $\hbar$ -curves for  $f(\zeta)$ ,  $g(\zeta)$ ,  $\theta(\zeta)$  and  $\phi(\zeta)$  are plotted in the ranges of  $-0.25 \leq \hbar \leq 0.00$ ,  $-0.35 \leq \hbar \leq 0.10$ ,  $-0.20 \leq \hbar \leq 0.00$  and  $-0.30 \leq \hbar \leq 0.10$  in Figs. (2-5) respectively.

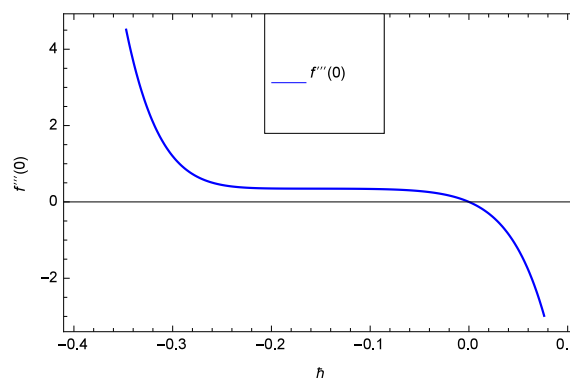


Figure 2:  $\hbar$  curve of  $f(\zeta)$ .

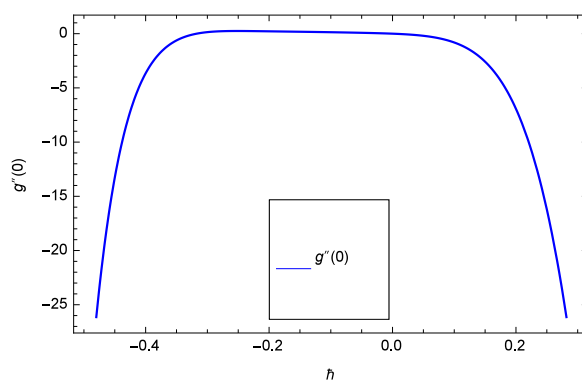


Figure 3:  $\hbar$  curve of  $g(\zeta)$ .

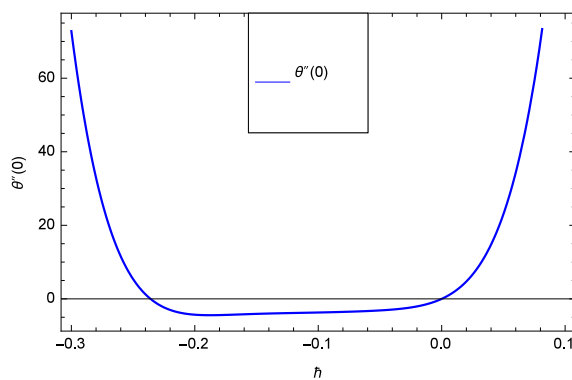


Figure 4:  $\hbar$  curve of  $\theta(\zeta)$ .

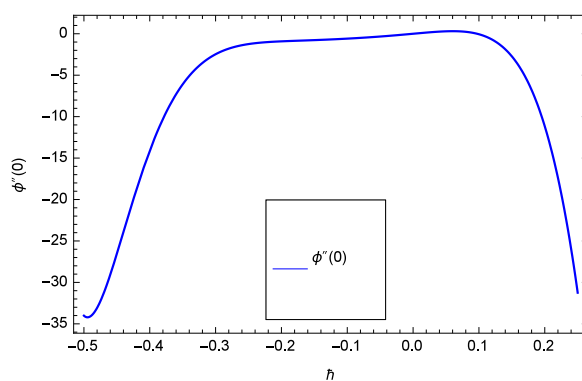


Figure 5:  $\hbar$  curve of  $\phi(\zeta)$ .

#### 4.1. Velocity Profile

Hall current is generated by the application of strong magnetic field to the boundary layer flow in the present problem. Boundary layer fluid motion decreases through the resistance offered by of magnetic field of high intensity since the magnetic field is applied in perpendicular direction to the flow. The magnetic field overcomes the flow regime. When the applied magnetic field is strong then the Hall effect generates an electric current to the flow in a side perpendicular to both the electric and magnetic fields which communicates with the applied magnetic field to produce a transverse flow of the fluid. Hall effect creates an extra flow in the transverse side, therefore it considerably affects the boundary layer flow features in the channel.

In the present problem one of the most important quantity is the layer thickness. The present boundary layer flow is relying on the thin film fluid parameter  $\beta$ . From Fig. 6, it appears that the velocity receives enhancement with dissimilar values of film size parameter  $\beta$ . As the thickness of the fluid film grows large, the speed of the boundary layer flow also rises which develops further by the favor of gravity force. Increasing thickness of the fluid film increases the mass of the boundary layer, consequently boundary layer flow becomes fast. The Hall parameter  $m$  plays a significant contribution in the boundary layer flow which is seen in Fig. 7. The axial velocity  $f(\zeta)$  tends to increase by increasing the Hall parameter  $m$ . The fact

is that Hall force pushes the fluid molecules in  $z$ -direction. The MHD dragging force -  $\frac{M(1 + \wedge\theta)(f' + mg)}{1 + m^2}$

in Eq. (16) becomes less in amount with rising quantities of  $m$  yielding an acceleration in the primary flow which generates the increment in the primary velocity  $f(\zeta)$ . Figure 8 depicts that the non-dimensional velocity  $f(\zeta)$  profile mitigates for the increasing flow quantities of second-grade fluid parameter  $\gamma_1$ . Incremental quantities of non-Newtonian parameter  $\gamma_1$  increase viscoelastic behaviors which are used to decrease the flow. When the values of second-grade fluid parameter  $\gamma_1$  increase the resistivity forces of the fluid increase consequently flow is hardly generated because force of attraction among liquid molecules is high. Figure 9 provides the role of magnetic field parameter  $M$ . For the high values of  $M$ , there exists an enough decrement in the axial velocity  $f(\zeta)$ . The axial motion is too much weakened for the excessive amount of  $M$ . The MHD

dragging factor -  $\frac{(1 + \wedge\theta)M(f' + mg)}{1 + m^2}$  in Eq. (16) shows the clear coupling of  $M$  with other factors like  $\wedge$ ,  $\theta$ ,  $f'$ ,  $m$  and  $g$  which describe that for high values of  $M$  and smaller or fixed values of  $m$ , the dragging force is enhanced sufficiently. Further, it is concluded that the axial velocity  $f(\zeta)$  always negative to any quantity of  $M$ , so the resulting effect of  $M$  leads to a decreasing behavior of motion.

An interesting phenomenon due to the increase in Hall parameter  $m$  for the secondary flow distribution is shown in Fig. 10. The transverse velocity  $g(\zeta)$  in secondary flow decreases consistently as the parameter  $m$  enhances and attains the lowest value when  $m = 1.00$ . The term  $\frac{1}{1+m^2}$  can be explored to deduce different conclusions about the Hall effect. Particularly, If  $m = 0$ , then the flow becomes two dimensional. So due to Hall effect the flow is three dimensional. The making of three dimensional study from two dimensional study is due to the application of strong applied magnetic field whose effect can be seen in Fig. 11. The

MHD dragging power -  $\frac{M(1 + \wedge\theta)(g - mf')}{1 + m^2}$  in Eq. (17) has two constituents *i. e.* non-negative constituent  $g(\zeta)$  and the negative constituent  $f(\zeta)$ . When the constituent  $f(\zeta)$  becomes positive through the multiple of -  $\frac{M(1+\wedge\theta)}{1+m^2}$  factor *i. e.* when it has the form  $\frac{M(1 + \wedge\theta)(mf')}{1 + m^2}$  (positive). In such situation, the transverse velocity  $g(\zeta)$  becomes strong due to axial velocity  $f(\zeta)$ . Furthermore if in the meantime  $M$  takes part for the rising positive values, then the transverse velocity  $g(\zeta)$  is distinctively high.

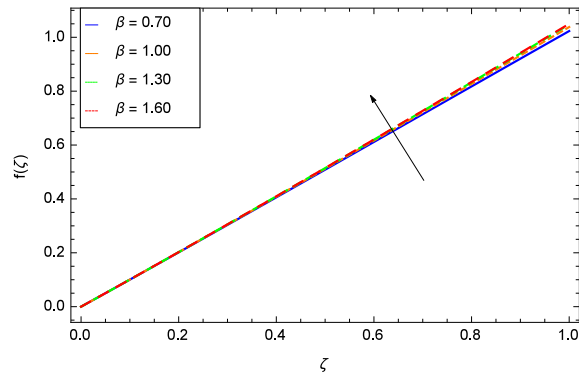


Figure 6: Axial velocity  $f(\zeta)$  for different values of  $\beta$ .

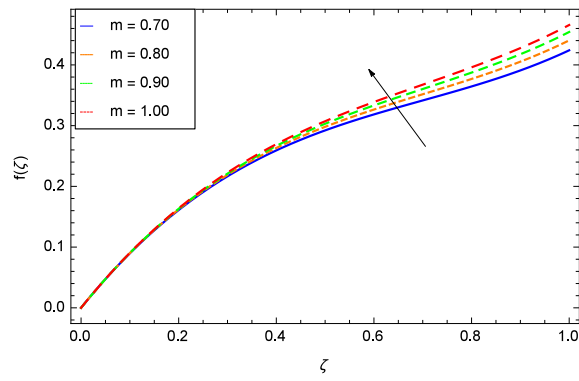


Figure 7: Axial velocity  $f(\zeta)$  for different values of  $m$ .

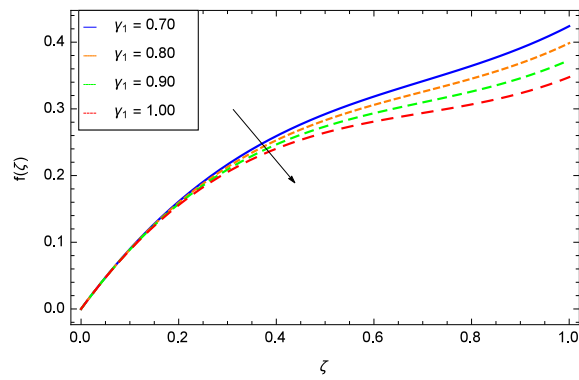


Figure 8: Axial velocity  $f(\zeta)$  for different values of  $\gamma_1$ .

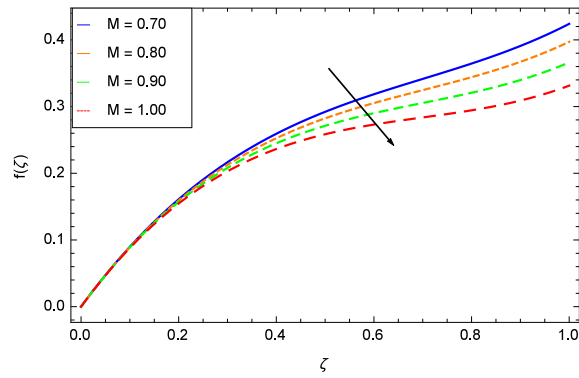


Figure 9: Axial velocity  $f(\zeta)$  for different values of  $M$ .

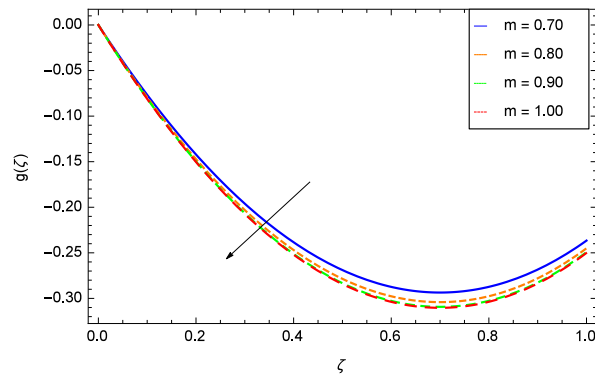


Figure 10: Transverse velocity  $g(\zeta)$  for different values of  $m$ .

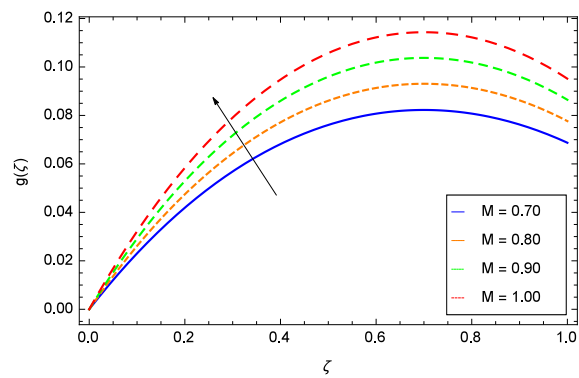


Figure 11: Transverse velocity  $g(\zeta)$  for different values of  $M$ .

#### 4.2. Temperature Profile

Temperature profile  $\theta(\zeta)$  is affected by each parameter. The effect of Hall parameter  $m$  on temperature  $\theta(\zeta)$  is displayed in Fig. 12. Temperature  $\theta(\zeta)$  rises for the high values of  $m$ . The MHD drag force  $-\frac{M(1 + \Lambda\theta)(f' + mg)}{1 + m^2}$  in Eq. (16) contains the term  $m$ . In numerator  $m$  has linear and in denominator  $m$  has the quadratic form. So if  $m$  is increased then  $m$  in denominator comparatively exerts a much influence on the drag force. Figure 13 shows the variable property of fluid showing the influence of viscosity parameter  $\Lambda$ . The parameter  $\Lambda$  decreases the temperature  $\theta(\zeta)$  due to the absorption of viscous forces. The reason is that by increasing viscosity, the cohesive and adhesive forces come into play and enhanced which absorb the heat. These forces are very strong and capture the liquid atoms/molecules firmly. Non-Newtonian liquids like second-grade, third-grade *etc.* are more viscous compared to that of Newtonian liquids. Due to strong attractive forces among the atoms and molecules too much heat is transferred into the fluid. This heat is used to make weaken the viscous forces. By increasing temperature the cohesive and adhesive forces of the liquid become weak consequently, thickness of the fluid decreases. The other variable fluid property is the thermal conductivity whose parameter  $\varepsilon$  is lying in Fig. 14 which reveals that heating conductivity of the liquid is enhanced for increasing temperature  $\theta(\zeta)$ . The reason is that temperature and thermal conduction of the liquid are interrelated to one another positively. Increasing one quantity, increases the other. Figure 15 shows that temperature decreases against the rising values of Dufour number. The reason is that diffusion thermal effect normally affects the fluid temperature greatly.

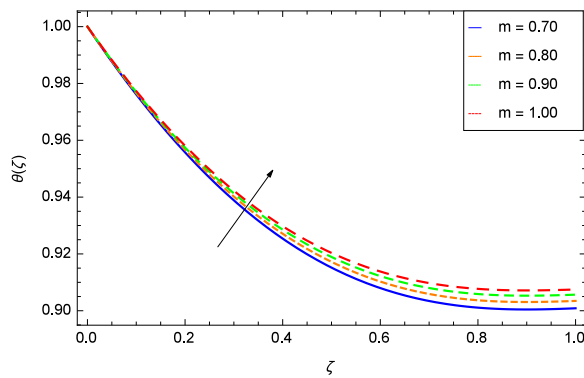


Figure 12: Temperature  $\theta(\zeta)$  for different values of  $m$ .

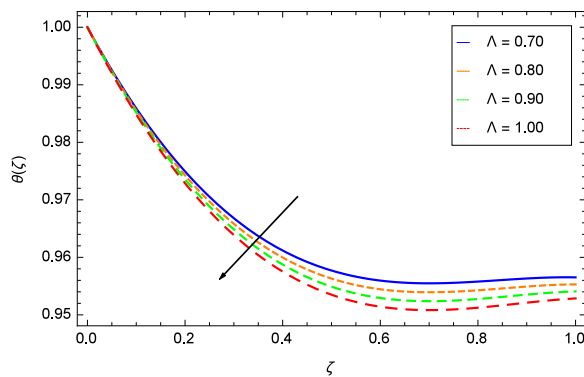


Figure 13: Temperature  $\theta(\zeta)$  for different values of  $\Lambda$ .

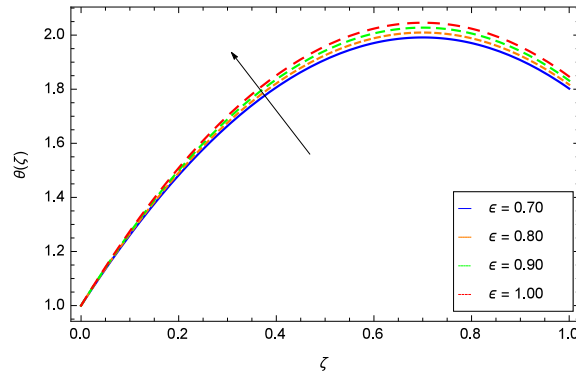


Figure 14: Temperature  $\theta(\zeta)$  for different values of  $\epsilon$ .

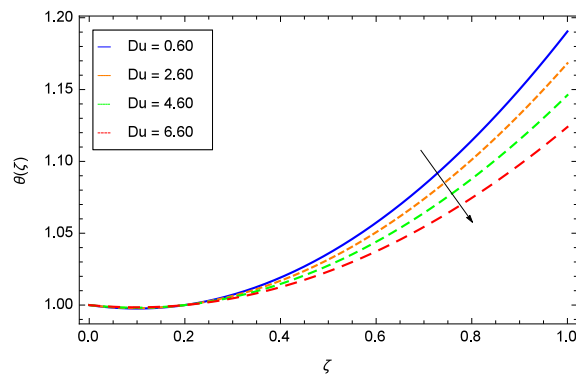


Figure 15: Temperature  $\theta(\zeta)$  for different values of  $Du$ .

### 4.3. Concentration Profile

Figure 16 is prepared for the pertinent parameter  $\tau$ . It shows that the non-dimensional concentration  $\phi(\zeta)$  profile becomes low when the thermophoretic parameter  $\tau$  grows high. The reason is that the greater quantities of thermophoretic parameter  $\tau$  reduce the size of concentration boundary layer. In fact the rising quantities of  $\tau$  bear depreciation in the concentration amount consequently, concentration  $\phi(\zeta)$  profile resumes minimum value. The effect of Soret number  $Sr$  on concentration  $\phi(\zeta)$  profile is depicted in Fig. 17, showing that concentration  $\phi(\zeta)$  amplifies when the parameter  $Sr$  rises. The reason is that an increment in  $Sr$  decreases the difference of temperatures between the surface and the ambient fluid as a result enhancements in the viscosity occur and therefore concentration  $\phi(\zeta)$  accelerates. By the increase of Soret number  $Sr$  the temperature difference between hot and surrounding fluid increases, so the temperature rises, consequently concentration  $\phi(\zeta)$  increases. Figure 18 shows that by making positive variation in the values of Schmidt number  $Sc$ , the depreciation of non-dimensional concentration  $\phi(\zeta)$  profile takes place. The definition of Schmidt number  $Sc$  attributes that an increase in  $Sc$  means lower molecular diffusivity, hence the concentration boundary layer reduces.

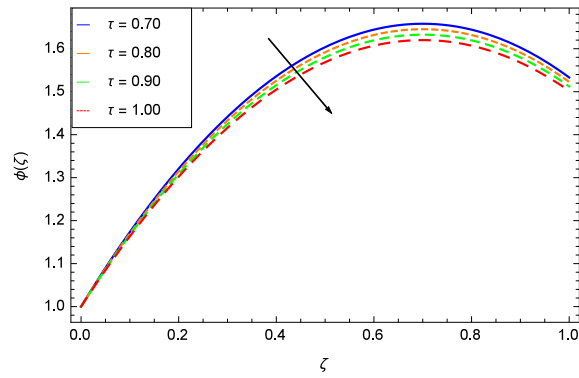


Figure 16: Concentration  $\phi(\zeta)$  for different values of  $\tau$ .

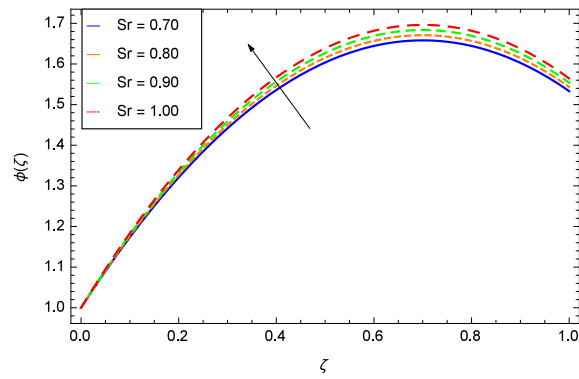


Figure 17: Concentration  $\phi(\zeta)$  for different values of  $Sr$ .

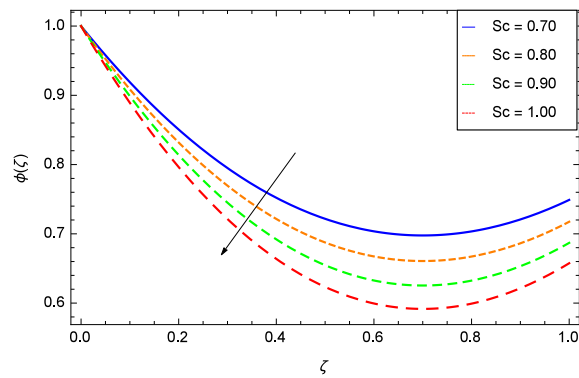


Figure 18: Concentration  $\phi(\zeta)$  for different values of  $Sc$ .

## 5. Conclusions

The study investigates the magnetohydrodynamic two dimensional boundary layer heat and mass transfer flow of a thin film second-grade fluid with temperature dependent viscosity and thermal conductivity past a stretching sheet in the regime of high intensified magnetic field. The main theme is about the transforming of two dimensional study into three dimensional space. The solution of the problem has been made through Homotopy Analysis Method (HAM). From the given figures, it is clear that various parameters have profound effects on the heat and mass transfer thin film flow.

## Competing Interests

The author declare that he has no competing interests.

## Acknowledgments

The author is thankful to the honorable reviewer for his excellent comments and suggestions to improve the quality of the manuscript.

The author would like to acknowledge the Higher Education Commission (HEC) Pakistan for providing the technical and financial support.

## References

- [1] N. S. Khan, T. Gul, S. Islam, A. Khan, Z. Shah, Brownian motion and thermophoresis effects on MHD mixed convective thin film second-grade nanofluid flow with Hall effect and heat transfer past a stretching sheet, *Journal of Nanofluids*, 6 (2017) 812–829, <https://dx.doi.org/10.1166/jon.2017.1383>.
- [2] M. Rafiq, H. Yasmin, T. Hayat, F. Alsaadi, Effects of Hall and ion-slip on the peristaltic transport of nanofluid: A biomedical application, *Chinese Journal of Physics*, (2019).
- [3] N. S. Khan, T. Gul, S. Islam, W. Khan, Thermophoresis and thermal radiation with heat and mass transfer in a magnetohydrodynamic thin film second-grade fluid of variable properties past a stretching sheet, *European Physical Journal Plus*, 132 (2017) 11, <https://dx.doi.org/10.1140/epjp/i2017-11277-3>.
- [4] M. Filippini, P. Alotto, G. Glehn, K. Hameyer, Magnetic transmission gear finite element simulation with iron pole hysteresis, 16 (2018) 105-110, doi: 10.1515/phys-2018-0017.
- [5] N. S. Khan, T. Gul, S. Islam, I. Khan, A. M. Alqahtani, A. S. Alshomrani, Magnetohydrodynamic nanoliquid thin film sprayed on a stretching cylinder with heat transfer, *Journal of Applied Sciences*, 7 (2017) 271.
- [6] M. R. Hajmohammadi, M. H. H. M. Ali, Effects of the magnetic field on the cylindrical Couette flow and heat transfer of a nanofluid, *Physica A Statistical Mechanics and its Applications*, (2019).
- [7] M. Bilal, M. Ramzan, Hall current effect on unsteady rotational flow of carbon nanotubes with dust particles and nonlinear thermal radiation in Darcy-Forchheimer porous media, *Journal of Thermal Analysis and Calorimetry*, (2019).
- [8] B. Fersadou, H. Kahalerras, W. Nessab, D. Hammoudi, Effect of magnetohydrodynamics on heat transfer intensification and entropy generation of nanofluid flow inside two interacting open rectangular cavities, *Journal of Thermal Analysis and Calorimetry*, (2019).
- [9] N. S. Khan, S. Zuhra, Boundary layer flow and heat transfer in a thin film second-grade nanoliquid embedded with graphene nanoparticles, *Advances in Mechanical Engineering*, 11(11) (2019) 1–11, <https://dx.doi.org/10.1177/1687814019884428>.
- [10] M. Atashafrooz, The effects of buoyancy force on mixed convection heat transfer of MHD nanofluid flow and entropy generation in an inclined duct with separation considering Brownian motion effects, *Journal of Thermal Analysis and Calorimetry*, (2019).
- [11] Z. Palwasha, N. S. Khan, Z. Shah, S. Islam, E. Bonyah, Study of two-dimensional boundary layer thin film fluid flow with variable thermophysical-properties in three dimensions space, *AIP Advances* 8 (2018) 105318, <https://dx.doi.org/10.1063/1.5053808>.
- [12] M. Khan, T. Salahuddin, M. Y. Malik, F. Khan, Arrhenius activation in MHD radiative Maxwell nanoliquid flow along with transformed internal energy, *European Physical Journal Plus*, 134 (2019) 198.
- [13] S. Zuhra, N. S. Khan, S. Islam, Magnetohydrodynamic second grade nanofluid flow containing nanoparticles and gyrotactic microorganisms, *Computational and Applied Mathematics* 37 (2018), 6332–6358. <https://dx.doi.org/10.1007/s40314-018-0683-6>.
- [14] O. F. Bidemi, M. S. S. Ahamed, Soret and Dufour effects on unsteady Casson magneto-nanofluid flow over an inclined plate embedded in a porous medium, *World Journal of Engineering*, 16 (2) (2019) 260–2274.
- [15] N. S. Khan, S. Zuhra, Z. Shah, E. Bonyah, W. Khan, S. Islam, Slip flow of Eyring-Powell nanoliquid film containing graphene nanoparticles, *AIP Advances* 8 (2019) 115302, <https://dx.doi.org/10.1063/1.5055690>.
- [16] Y. S. Daniel, Z. A. Aziz, Z. Ismail, A. Bahar, F. Salah, Slip role for unsteady MHD mixed convection of nanofluid over stretching sheet with thermal radiation and electric field, *Indian Journal of Physics*, (2019).
- [17] M. R. Zangoee, Kh. Hosseinzadeh, D. D. Ganji, Hydrothermal analysis of MHD nanofluid (TiO<sub>2</sub>-GO) flow between two radiative stretchable rotating disks using AGM, *Case Studies in Thermal Engineering*, (2019).

- [18] S. Zuhra, N. S. Khan, Z. Shah, S. Islam, E. Bonyah, Simulation of bioconvection in the suspension of second grade nanofluid containing nanoparticles and gyrotactic microorganisms. *AIP Advances* 8, (2018) 105210. <https://dx.doi.org/10.1063/1.5054679>
- [19] N. S. Khan, P. Kumam, P. Thounthong, Renewable energy technology for the sustainable development of thermal system with entropy measures. *International Journal of Heat and Mass Transfer* 145 (2019) 118713. <https://dx.doi.org/10.1016/j.ijheatmasstransfer.2019.118713>
- [20] Z. Palwasha, S. Islam, N. S. Khan, H. Ayaz, Non-Newtonian nanoliquids thin film flow through a porous medium with magnetotactic microorganisms. *Applied Nanoscience* 8 (2018) 1523–1544. <https://dx.doi.org/10.1007/s13204-018-0834-5>
- [21] N. S. Khan, Z. Shah, S. Islam, I. Khan, T. A. Alkanhal, I. Tlili, Entropy generation in MHD mixed convection non-Newtonian second-grade nanoliquid thin film flow through a porous medium with chemical reaction and stratification. *Entropy* 21 (2019) 139. <https://dx.doi.org/10.3390/e21020139>
- [22] N. S. Khan, S. Zuhra, Q. Shah, Entropy generation in two phase model for simulating flow and heat transfer of carbon nanotubes between rotating stretchable disks with cubic autocatalysis chemical reaction. *Applied Nanoscience* 9 (2019) 1797–1822. <https://dx.doi.org/10.1007/s13204-019-01017-1>
- [23] N. S. Khan, Bioconvection in second grade nanofluid flow containing nanoparticles and gyrotactic microorganisms. *Brazilian Journal of Physics* 43 (4) (2018) 227–241. <https://dx.doi.org/10.1007/s13538-018-0567-7>
- [24] S. Benbernou, A note on the regularity criterion in terms of pressure for the Navier-Stokes equations, *Applied Mathematics Letters*, 22 (2009) 1438–1443.
- [25] S. Gala, Q. Liu, M. A. Ragusa, Logarithmically improved regularity criterion for the nematic liquid crystal flows in  $B_{\infty, \infty}^{-1}$  space, *Computers and Mathematics with Applications*, 65 (2013) 1738–1745.
- [26] S. Benbernou, M. A. Ragusa, M. Terbeche, A logarithmically improved regularity criterion for the MHD equations in terms of one directional derivative of the pressure, *Applicable Analysis*, 96 (2016) 2140–2148, <https://dx.doi.org/10.1080/00036811.2016.1207246>.
- [27] S. Gala, M. A. Ragusa, Logarithmically improved regularity criteria for supercritical quasi-geostrophic equations in Orlicz-Morrey spaces, *Electronic Journal of Differential Equations*, 2016 (137) (2016) 1–7.
- [28] S. Gala, M. A. Ragusa, Logarithmically improved regularity criteria for the Boussinesq equations in Besov spaces with negative indices, *Applicable Analysis*, 95 (2016) 1271–1279.
- [29] S. Gala, Z. Guo, M. A. Ragusa, A remark on the regularity criterion of Boussinesq equations with zero heat conductivity, *Applied Mathematics Letters*, 22 (2014) 70–73.
- [30] M. Mehdene, S. Gala, Z. Guo, M. A. Ragusa, Logarithmical regularity criterion of the three-dimensional Boussinesq equations in terms of the pressure, *Zeitschrift fur Angewandte Mathematik und Physik* 67 (2016).
- [31] S. Gala, M. A. Ragusa, A logarithmic regularity criterion for the two-dimensional MHD equations, *Journal of Mathematical Analysis and Applications*, 444 (2016) 1752–1758, <https://dx.doi.org/10.1016/j.jmaa.2016.07.001>.
- [32] N. S. Khan, T. Gul, S. Islam, W. Khan, I. Khan, L. Ali, Thin film flow of a second-grade fluid in a porous medium past a stretching sheet with heat transfer, *Alexandria Engineering Journal* 57 (2017) 1019–1031, <https://dx.doi.org/10.1016/j.aej.2017.01.036>.
- [33] S. Zuhra, N. S. Khan, M. A. Khan, S. Islam, W. Khan, E. Bonyah, Flow and heat transfer in water based liquid film fluids dispensed with graphene nanoparticles, *Results in Physics* 8 (2018) 1143–1157. <https://dx.doi.org/10.1016/j.rinp.2018.01.032>
- [34] N. S. Khan, S. Zuhra, Z. Shah, E. Bonyah, W. Khan, S. Islam, A. Khan, Hall current and thermophoresis effects on magneto-hydrodynamic mixed convective heat and mass transfer thin film flow. *Journal of Physics Communication* 3 (2019) 035009. <https://dx.doi.org/10.1088/2399-6528/aaf830>
- [35] N. S. Khan, T. Gul, P. Kumam, Z. Shah, S. Islam, W. Khan, S. Zuhra, A. Sohail, Influence of inclined magnetic field on Carreau nanoliquid thin film flow and heat transfer with graphene nanoparticles, *Energies* 12 (2019) 1459. <https://dx.doi.org/10.3390/en12081459>.
- [36] N. S. Khan, T. Gul, M. A. Khan, E. Bonyah, S. Islam, Mixed convection in gravity-driven thin film non-Newtonian nanofluids flow with gyrotactic microorganisms, *Results in Physics* 7 (2017) 4033–4049, <https://dx.doi.org/10.1016/j.rinp.2017.10.017>.
- [37] S. J. Liao, *Homotopy Analysis Method in Nonlinear Differential Equations*, Higher Education Press Beijing and Springer-Verlag Berlin Heidelberg, 2012.